Microchimica Acta (2018) 185: 512
https://doi.org/10.1007/s00604-018-3044-7

ORIGINAL PAPER

An array consisting of glycosylated quantum dots conjugated to MoS_2 nanosheets for fluorometric identification and quantitation of lectins and bacteria

Haimei Yang[1] · Xu Jie[1] · Lu Wang[1] · Yue Zhang[1] · Min Wang[1] · Weili Wei[1]

Received: 19 June 2018 / Accepted: 6 October 2018 / Published online: 20 October 2018

Abstract

A fluorescent array based on the use of saccharide-functionalized multicolored quantum dots (s-QDs) and of 4-mercaptophenylboronic acid-functionalized MoS_2 nanosheets (PBA-MoS_2) was constructed for multiple identification and quantitation of lectins and bacteria. In this array, the fluorescence of the s-QDs is quenched by the PBA-MoS_2 nanosheets. In the presence of multiple lectins, s-QDs differentially detach from the surface of PBA-MoS_2 nanosheets, producing distinct fluorescence response patterns due to both quenching and enhancement of fluorescence. By analyzing the fluorescence responses with linear discriminant analysis, multiple lectins and bacteria were accurately identified with 100% accuracy. The limits of detection of *Concanavalin A*, *Pisum sativum* agglutinin, *Peanut* agglutinin, and *Ricius communis I* agglutinin are as low as 3.7, 8.3, 4.2 and 3.9 nM, respectively. The array has further been evidenced to be potent for distinguishing and quantifying different bacterial species by recognizing their surface lectins. The detection limits of *Escherichia coli* and *Enterococcus faecium* are 87 and 66 cfu mL^{-1}, respectively.

Keywords Fluorescence · Linear discriminant analysis · Saccharide binding · Milk sample · Multiple analysis

Introduction

Lectins are nonimmunogenic carbohydrate-recognizing proteins that bind specifically and reversibly to different saccharide moieties [1]. They perform recognition on both the cellular and molecular level, and are highly associated with many physiological and pathological events in living organisms, such as cell recognition and adhesion, cancer metastasis, bacterial and viral infections [2, 3]. Hence, identification of these lectins-based interactions holds great hopes for understanding the molecular mechanisms of the relevant biological pathways, which further benefits the development of drugs for cancer theranostics, bacterial detection and invasion prevention. Currently, various approaches have been developed for lectin detection based on lectin-carbohydrate recognition, including fluorescent [4], electrochemical [5], surface enhanced Raman scattering (SERS) [6], colorimetric [7, 8] methods. Although these methods are effective, most of them are time-consuming, expensive, and only capable of detecting one specific lectin [9]. Actually, various types of lectins usually coexist in real samples such as the surface [10] of cancer cells, bacteria, virus; and multiple lectin-carbohydrate interactions occur simultaneously to control cellular event. For instance,the *Escherichia coli* (*E. coli*) surface contains two types of lectins, type 1 and type 2 fimbrial lectins, which are mannose and galactose moieties specific, respectively [11]. In addition, a same saccharide often showed a broad range of binding affinities to several types of lectins, and vice versa [12]. Consequently, the aforementioned lectin detection methods [5–8] are not suitable for detecting multiple lectins simultaneously. A few good attempts have been carried out for the purpose of multiple detection lectins [12, 13]. However, the patterned colorimetric signals for different lectins were subtle and indistinguishable by eye, and they did not carry out real sample analysis. In this regard, for a more

Electronic supplementary material The online version of this article (https://doi.org/10.1007/s00604-018-3044-7) contains supplementary material, which is available to authorized users.

✉ Min Wang
wang_min@cqu.edu.cn

✉ Weili Wei
wlwei@cqu.edu.cn

[1] School of Pharmaceutical Sciences, Chongqing University, Chongqing 401331, People's Republic of China

comprehensive understanding of biological events, it is essential to achieve the identification of multiple lectins rather than a single lectin with good sensitivity, specificity, and visible discrimination.

Alternatively, the sensor arrays, which are composed of a series of receptor units with cross-reactivity toward different analytes, have been widely used for simultaneously multicomponent identification and analysis with the assistance of statistical methods [14]. The classical semiconductor quantum dots (QDs) are ideal signal probes for a sensor array due to their unique photoluminescent properties like colorful emission, high luminescent quantum yields and photostability [15]. The QDs are usually functionalized with specific ligands to recognize different analytes. Then signal transducers are applied to transduce recognition events into distinct signal response patterns for different analytes. Various nanoquenchers such as metal nanoparticles, and metal oxide nanoparticles have been integrated as fluorescent signal transducers [16]. Besides, two-dimensional (2D) MoS_2 nanosheets should be superior nanoquenchers due to their unique physiochemical properties such as layered 2D structure and large special surface area [17]. Accordingly, MoS_2 nanosheets have been employed as a sensing platform for the detection of nucleic acids [18], metal ions [19], and other small molecules [20]. However, simultaneous multiple detection of analytes (e.g. lectins, bacteria) has not been reported by using the visible pattern generating s-QDs/MoS_2 nanosheets conjugation array.

Herein, a fluorescent array for simultaneous detection of multiple lectins and demonstrated its potential in the diagnosis of bacterial infections based on 4-mercaptophenylboronic acid-functionalized MoS_2 (PBA-MoS_2) nanosheets and three saccharide-functionalized CdSe/ZnS QDs (s-QDs) (Scheme 1) was constructed. In the presence of PBA-MoS_2 nanosheets, the s-QDs can attach onto the nanosheets via the formation of dynamic phenylboronate esters between PBA and *cis*-vicinal diol moieties of the saccharides of s-QDs. Consequently, the fluorescence of s-QDs should be quenched by PBA-MoS_2 nanosheets. Interestingly, once the lectins coexisted, s-QDs would competitively bind to lectins, resulting detachment of s-QDs from nanosheets and fluorescence recovery. Based on this principle, the QDs with green (520 nm, QD_{520}), yellow (580 nm, QD_{580}), and red (660 nm, QD_{660}) emission were modified with mannose (Man-QD_{520}), glucose (Glu-QD_{580}), and galactose (Gal-QD_{660}) moieties, respectively. The three s-QDs, Man-QD_{520}, Glu-QD_{580} and Gal-QD_{660}, with different emission color and lectin binding capability were conjugated with PBA-MoS_2 nanosheets, and employed as cross-reactive fluorescent array for multiple recognition and quantitation of lectins with excellent accuracy (Scheme 1b). This method can also be used for identification of bacteria by recognition of their surface lectins.

Experimental

Materials and reagents

The bulk MoS_2 powder and *n*-butyllithium (*n*-BuLi) were obtained from Aladdin Reagent Co., Ltd. (Shanghai, China, www.aladdin-e.com). Mannose (Man), glucose (Glu), and galactose (Gal) were purchased from Adamas-Beta (Shanghai, China, www.adamas-beta.com). All core-shell CdSe/ZnS QDs emitting green (520 nm, QD_{520}), yellow (580 nm, QD_{580}), and red (660 nm, QD_{660}) light were purchased from XingZi New Material Technology Development Co., Ltd. (Shanghai, China, www.xznanomat.com). 4-mercaptophenylboronic acid (PBA-SH) and five lectins, *Concanavalin A* (ConA), *Pisum sativum* agglutinin (PSA), *Peanut* agglutinin (PNA), *Ricinus communis I* agglutinin (RCA), and *Wheat germ* agglutinin (WGA) were purchased from Sigma-Aldrich (Shanghai, China, www.sigmaaldrich.com). Five bacterial strains, *Escherichia coli* (*E. coli), Enterococcus feacalis (E. faecalis), Enterococcus faecium (E. faecium), Staphylococcus aureus (S. aereus),* and *Bacillus subtilis (B. sublitis)* were purchased from China Forestry Culture Collection Center (Beijing, China, www.accc.org.cn). All bacterial-culture related reagents were purchased from Sangon Biotech Co., Ltd. (Shanghai, China, www.sangon.com). All reagents were of analytical reagent grade or above and used as received without further purification. All aqueous solutions were prepared using ultrapure water (18.25 MΩ cm, milli-Q, Millipore).

Instrumentation

Fluorescence measurements were performed on a Shimadzu RF-5301PC spectrophotometer equipped with a Xenon lamp excitation source. Fourier transform infrared (FT-IR) spectroscopy measurements were performed on a BRUKER Vertex 70 FT-IR spectrometer with KBr pellets in the 400–4000 cm^{-1} region. ^{1}H and ^{13}C NMR spectra were recorded on an Agilent 400MR DD2 400-MHz spectrometer. Electrospray ionization-mass spectrometry (ESI-MS) analysis was conducted on an ACQUITY SQD single quadrupole high performance liquid chromatography-mass spectrometry (HPLC-MS) system (Waters, USA). Transmission electron microscopy (TEM) images were obtained on a Philips Tacnai G2 20 S-TWIN trans-mission electron microscope operating at 200 kV. Atomic force microscope (AFM) measurements were carried out on a Veeco Dimentional 3100.

Fabrication of s-QDs/MoS_2 nanosheets conjugation array

For construction of s-QDs/MoS_2 nanosheets conjugation array, each s-QDs (Man-QD_{520}, Glu-QD_{580}, and Gal-QD_{660})

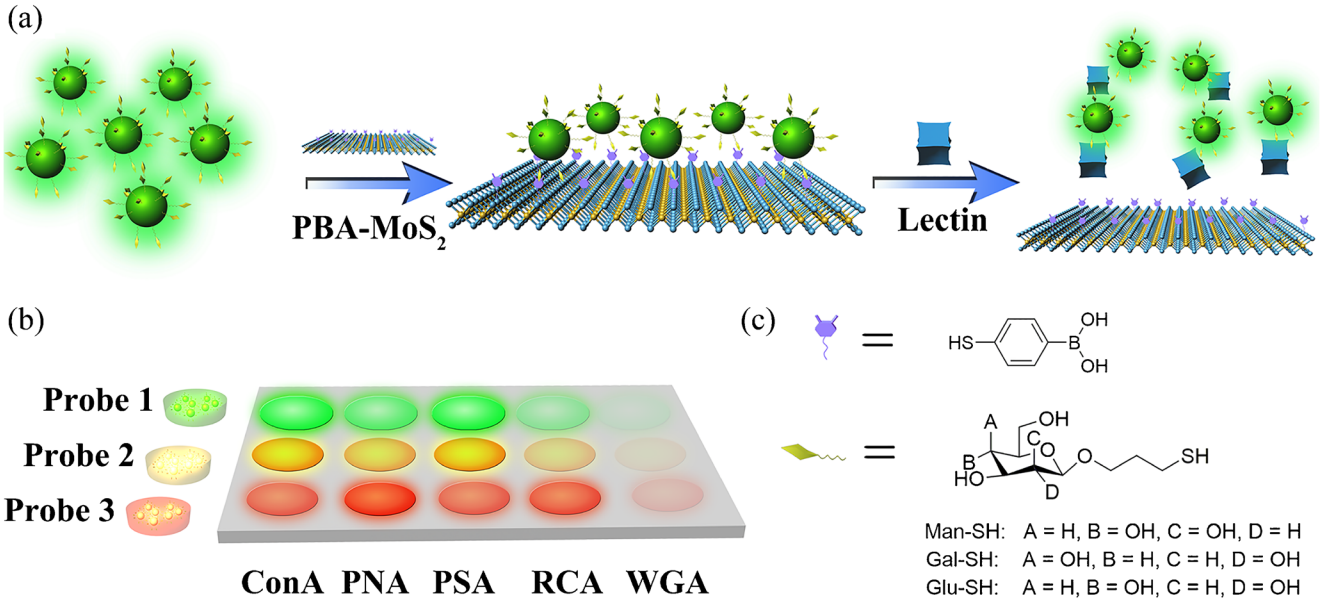

Scheme 1 **a** Schematic illustration of the design rationale for lectin detection. **b** Construction of fluorescent array by employing Man-QD_{520} (Probe 1), Glu-QD_{580} (Probe 2), and Gal-QD_{660} (Probe 3) as three signal probes. **c** Molecular structures of saccharide derivatives for QDs modification

and PBA-MoS_2 nanosheets with desired concentration were mixed with phosphate buffer (10 mM, pH = 7.2), respectively. The final concentrations of s-QDs and PBA-MoS_2 nanosheets were 10 μg mL^{-1} and 0.1 mg mL^{-1}, respectively. After incubation for 15 min, the fluorescence spectra in the absence of lectins (or bacteria) were measured at an excitation wavelength of 380 nm, and the fluorescence intensities at 520, 580, and 660 nm were recorded (F_0). In the presence of a certain amount of lectin (or bacteria), the fluorescence intensity at the corresponding wavelength was measured as F. The variation of fluorescence intensity ($\Delta F = F - F_0$) was used for further statistical analysis.

Multiple sensing of lectins

Three kinds of s-QDs (50 μL, 30 μg mL^{-1}) were mixed with certain amount of lectins, respectively and incubated at room temperature for 3 h. Then 10 μL of PBA-MoS_2 nanosheets (1.5 mg mL^{-1}) was added to the above mixture and supplemented with 70 μL buffer (10 mM, containg 0.1 mM $Ca^{2+}$and 0.1 mM Mn^{2+}, pH = 7.2) to maintain 150 μL total fluid volumes and give the final lectins concentrations in the range of 30–480 nM. Finally, the fluorescence spectra were record after incubating the mixture for 15 min ($\lambda_{ex/em}$ = 380/520 nm, 380/580 nm, 380/660 nm).

Bacteria detection

As for bacteria sensing, a similar procedure was followed. Five bacterial strains (*E. coli, E. faecalis, E. faecium, S. aereus,* and *B. sublitis)* were cultured in Luria-Bertani (LB) medium (10 g L^{-1} tryptone, 5 g L^{-1} yeast extract and 10 g L^{-1} NaCl) at 37 °C overnight on the shaker of 180 rpm in the dark. The medium for *B. sublitis* strain culture should contain 0.2 g L^{-1} beef extract. For bacteria identification, bacteria were separated from the growth medium and suspended in buffer to achieve an optical density (OD) of 1.0 at 600 nm. 10 μL of the bacteria solution and 50 μL of s-QDs (30 μg mL^{-1}) disperse were incubated with 80 μL buffer for 2 h at 37 °C, the fluorescence spectra were recorded after adding 10 μL PBA-MoS_2 nanosheets (1.5 mg mL^{-1}) for 15 min ($\lambda_{ex/em}$ = 380/520 nm, 380/580 nm, 380/660 nm).

Quantitative detection of *E. coli* and *E. faecium*

For bacteria detection, 100 μL of various concentrations 0, 10, $10^{1.5}$, 10^2, 10^3, 10^4, 10^5, 10^6, 10^7, and 10^8 cfu mL^{-1} of *E. coli* and *E. faecium* were incubated with s-QDs (75 μg mL^{-1}, 20 μL), for 2 h at 37 °C in 20 μL of buffer. Then the PBA-MoS_2 nanosheets (1.5 mg mL^{-1}, 10 μL) were added and fluorescence spectra were recorded with the excitation of 380 nm.

Unknown sample identification

For detection of unknown samples, lectins and bacteria were prepared and tested as training matrix. We replicate each unknown sample three times, and the resulting fluorescence response patterns (ΔF) were tested by LDA and were ranked according to their Euclidean distances to the groups generated through the training matrix and returned the nearest samples to the respective groups.

Results and discussion

Choice of materials

The semiconductor QDs were chosen as fluorophores due to their colorful emission, high luminescent quantum yields, photostability and easier modification in comparison of organic dyes. Generally, various nanomaterials such as MoS_2 nanosheets, graphene oxide, reduced graphene oxide, and gold nanoparticles have been intensely studied as fluorescence quencher. In this work, we use MoS_2 nanosheets as the quencher based on two points: (1) the MoS_2 nanosheets can be readily decorated with functional ligands via Mo-S or S-S bonds, but the modification of the carbon-based graphene species is relatively difficult; (2) the two dimensional layered structure of MoS_2 nanosheets have much larger aspect area than the spherical gold nanoparticles. Therefore, the QDs-MoS_2 conjugates were chosen to construct the fluorescence array for lectin and bacteria analysis.

Characterization of PBA-MoS_2 nanosheets and s-QDs

MoS_2 nanosheets and PBA-MoS_2 nanosheets was prepared through Knirsch's method [21]. The details of preparation were shown in ESM. The morphology characteristic of MoS_2 and PBA-MoS_2 nanosheets were first investigated by AFM (Fig. S1, ESM). The bare MoS_2 nanosheets exhibited a lateral dimension in the range of 50–200 nm and an average height of 1.2 nm, which suggested that most of nanosheets consist of one to three MoS_2 layers (Fig. S1a, b, ESM). After functionalization with PBA-SH, the average height of PBA-MoS_2 nanosheets increased to an average of 1.5 nm (Fig. S1c, d, ESM), demonstrating that PBA-SH was attached on both surfaces of MoS_2 nanosheets. The successful functionalization of MoS_2 nanosheets were further confirmed by FT-IR spectra. As shown in Fig. S2 (ESM), the FT-IR spectra of bare MoS_2 and PBA-MoS_2 nanosheets were obviously different. In the spectrum of PBA-SH, the band at 2563 cm^{-1} was ascribed to the stretching vibration of S-H. The bands at 2924 cm^{-1} and 890 cm^{-1} were attributed to the stretching vibration and bending vibration of aromatic C-H, and the bands at 1604 cm^{-1} and 1370 cm^{-1} were assigned to the stretching vibration of aromatic C=C and the bending vibration of O-H, respectively. Consequently, the spectrum of PBA-MoS_2 nanosheets showed the characteristic bands at 2924 cm^{-1}, 1604 cm^{-1}, 1370 cm^{-1} and 890 cm^{-1}, which were inherited from PBA-SH. More importantly, the S-H band of PBA-SH disappeared, indicating the formation of S-Mo bond after modification. These results confirm that the phenylboronic moieties were covalently functionalized to MoS_2 nanosheets.

Mannose, glucose and galactose were thiolated according to a previously reported method with some modifications [22, 23]. The details of synthesis were shown in ESM. The thiolated mannose, glucose, and galactose were denoted as Man-SH, Glu-SH, and Gal-SH, respectively. The three QDs were commercially purchased. After modification with saccharides, all the three s-QDs (man-QD_{520}, glu-QD_{580}, and gal-QD_{660}) kept well mono-dispersion in water solution, indicating the surface of the QDs became hydrophilic due to the saccharide moieties. Fig. S3 (ESM) showed the typical TEM image of Man-QD_{520}, Glu-QD_{580}, and Gal-QD_{660} with average diameters of 8.07 ± 2 nm, 10.22 ± 2 nm, and 18.32 ± 3 nm, respectively. All appeared spherical particles with good monodispersity. The successful preparation of s-QDs was further confirmed by FT-IR spectra. Compared to the as-received QDs, the FT-IR spectra of s-QDs showed the typical vibration bands of C-H bond (1637 cm^{-1} and 1560 cm^{-1}) and C-O-C bond (1022 cm^{-1}) in carbohydrates (Fig. S4-S6, ESM). These results demonstrated that three types of s-QDs functionalized with different saccharides were successfully prepared.

Fluorescence titration

Before construction of fluorescent array, the quenching efficiency of PBA-MoS_2 nanosheets toward the Man-QD_{520}, Glu-QD_{580}, and Gal-QD_{660} was examined through fluorescence titration (Fig. 1). As shown in Fig. 1a–c, the fluorescence of all the three s-QDs gradually quenched with the increase of the concentration of the quencher PBA-MoS_2 nanosheets. With 0.1 mg mL^{-1} PBA-MoS_2 nanosheets, the fluorescence quenching rates ($[F_0\text{-}F]/F_0$) for Man-QD_{520}, Glu-QD_{580}, and Gal-QD_{660} were 53%, 43%, and 48%, respectively. Significantly, the fluorescence quenching of PBA-MoS_2 nanosheets to s-QDs (10 μg mL^{-1}) was visible in the absence and presence of PBA-MoS_2 nanosheets (0.3 mg mL^{-1}) (*inset* of Fig. 1d). To confirm the quenching mechanism, the absorbance spectrum of MoS_2 nanosheets measurement was recorded. As shown in Fig. S10, the MoS_2 nanosheets showed strong absorbance from UV to near-infrared, indicating the presence of energy transfer effect between PBA-MoS_2 nanosheets and s-QDs [19, 24]. The efficient quenching effect of the PBA-MoS_2 nanosheets was due to the close attachment of s-QDs to PBA-MoS_2 nanosheets, resulting in promoting efficient energy transfer between them. This also supports the sensing principle of this work as displayed in Scheme 1. In comparison, the quenching efficiency of the same concentration of bare MoS_2 nanosheets (without PBA) was less than 9% (Fig. S7, ESM). The results further confirmed that PBA modification endowed efficient quenching ability for PBA-MoS_2 nanosheets.

We then selected the proper titration point for this array. The value influences the dynamic range and response probability in the array. According to the fluorescence titration (Fig. 1d), a point about 50% quenching rate was selected on the titration curves in the consideration of following aspects. At this point, with the addition of analytes (lectins), the fluorescence was most possibly recovered due to competitive binding with s-QDs; and this point also allowed further

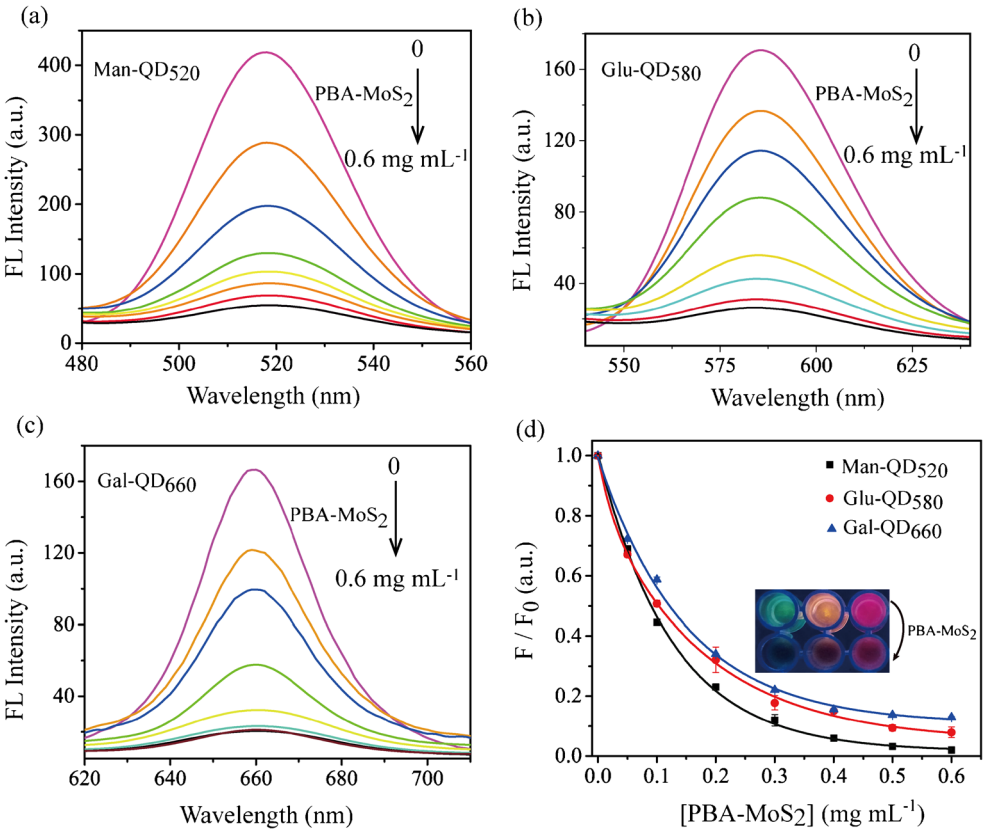

Fig. 1 **a**–**c** Fluorescence spectra of s-QDs (10 μg mL^{-1}), including (**c**) in the presence of increasing concentrations of PBA-MoS_2 nanosheets (The arrow: 0, 0.05, 0.1, 0.2, 0.3, 0.4, 0.5, and 0.6 mg mL^{-1} in sequence) upon the excitation at 380 nm. **d** Fluorescence titration curves of s-QDs with PBA-MoS_2 nanosheets; inset shows the s-QDs solutions (10 μg mL^{-1}) before and after the addition of PBA-MoS_2 nanosheets (0.3 mg mL^{-1}). $n = 3$

fluorescent quenching due to analytes induced aggregation or tighter attachment of s-QDs with PBA-MoS_2 nanosheets [4]. Therefore, points at ca. 50% quenching rate were set as signal readout for following assay. In this assay, the optimal concentration of PBA-MoS_2 nanosheets and s-QDs were 0.1 mg mL^{-1} and 10 μg mL^{-1}, respectively.

Simultaneous identification of lectins

Subsequently, the fluorescent array was established by mixing the corresponding s-QDs and PBA-MoS_2 nanosheets in aqueous solution to the final concentrations of 10 μg mL^{-1} and 100 μg mL^{-1}, respectively. As a proof-of-concept, five lectins (0.48 μM) with different saccharides binding ability, molecular weight (MW) and isoelectric point (pI) (Table S2, ESM) as the analytes. Corresponding fluorescence intensity of the Man-QD_{520}, Glu-QD_{580}, and Gal-QD_{660} at 520, 580, and 660 nm was recorded before and after adding different lectins. Fig. S8 shows the fluorescence changed by five lectins (0.48 μM), including ConA, PSA, PNA, RCA and WGA. Accordingly, different lectins resulted in obviously distinguishable fluorescent signal due to their different binding ability with different saccharides (Table S3, ESM). Next, the ability to simultaneous differentiation of multiple lectins (0.48 μM final concentration) was further investigated. With the fluorescence signal recorded, the signal change was defined as $\Delta F = F - F_0$, where F and F_0 are the intensity of fluorescence in the presence and absence of lectins. The differential signal changes in Fig. 2a indicate that these different signal responses can be used as an optical fingerprint for multiple lectin identification. Distinctly, fluorescence recovery was induced by ConA, PSA, PNA and RCA. For instance, the fluorescence of Man-QD_{520}/PBA-MoS_2 nanosheets conjugates gradually recovered within 10 min after the addition of Con A (Fig. S9, ESM). The kinetic deference clearly confirmed that Con A would competitively bind to s-QDs, resulting in s-QDs detached from PBA-MoS_2 nanosheets partly or completely and fluorescence recovery. Similar time-dependent fluorescence recovery behaviors were observed while the addition of PSA, PNA, and RCA. However, there was an exception that, the WGA induced fluorescence further quenching but not recovery. This can be explained in two aspects. On one hand, compared to ConA, PSA, PNA and RCA, WGA had no affinity with mannose, glucose and galactose moieties (Table S3, ESM), and thus it cannot make s-QDs detach from the surface of PBA-MoS_2 nanosheets. On the other hand, WGA is rich of amino groups (pI >9) that can promote the formation of phenylboronate esters between PBA and *cis*-vicinal diol moieties of the saccharides of s-QDs and further stabilizing the s-QDs/MoS_2 nanosheets conjugates [25]. The resultant fluorescence response patterns were qualitatively analyzed by linear discriminant analysis (LDA),

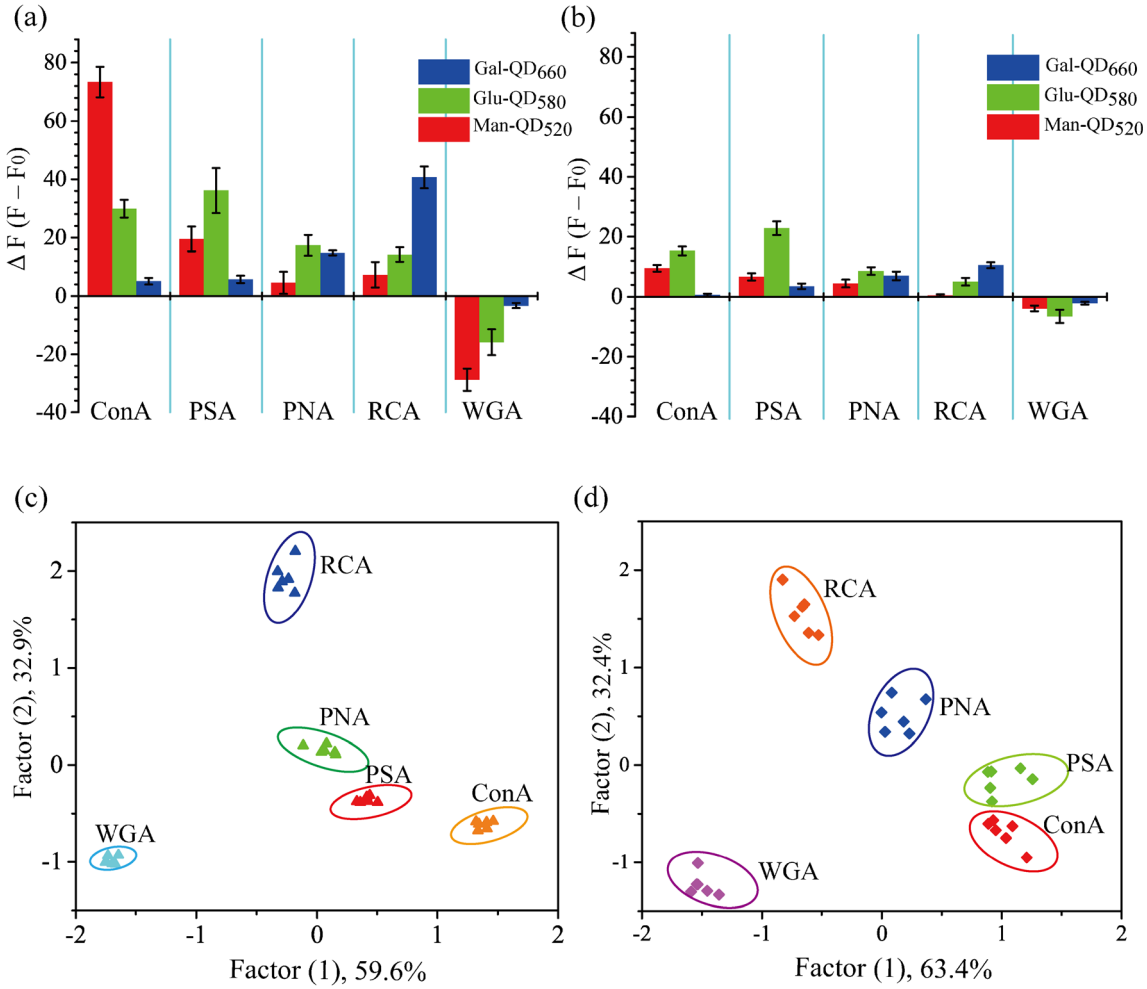

Fig. 2 **a**, **b** Fluorescence response patterns of the fluorescent array against 480 nM (**a**) and 48 nM (**b**) of five lectins (ConA, PSA, PNA, RCA and WGA). **c**, **d** Canonical score plot of 480 nM (**c**) and 48 nM (**d**) lectins via Linear discriminant analysis (LDA) signal patterns. $\Delta F = F - F_0$, where F and F_0 are the intensity of fluorescence in the presence and absence of lectins. $n = 6$

which is a powerful statistical technique and has been widely used in pattern recognition [24]. Based on this, six replicates were obtained for each lectins producing 90 test cases (3 probes ×5 lectins ×6 replicates) for each array, and the data were subjected to LDA to produce three canonical factors (59.6%, 32.9%, and 7.5%). The magnitude of canonical factor acts as a significant contribution from each dimension to indicate multiple axes of differentiation. The first two most significant discrimination factors were plotted in a two-dimensional (2D) model (Fig. 2c), all lectins were separated completely from each other without any overlap, demonstrating that they were effectively discriminated by the fluorescent array. In this 2D model, each point represents the response pattern of an individual lectin in the array. Consequently, the 30 fluorescence response patterns (5 lectins ×6 replicates) were distinguished as 5 distinct groups with 100% accuracy. The recognition efficiency was validated by identification of fifteen randomly unknown samples from our training matrix, all samples were correctly identified (Table S5, ESM). These results demonstrated that the array showed excellent identification accuracy to identify simultaneously multiple lectins.

Previous biosensor system can detect single lectin at nanomolar concentration [7, 26]. In this purpose, we further explored the ability of the method to identify multiple lectins at lower concentrations for potential practical application. Similar to the detection of 0.48 μM lectin, there still observed differential fluorescence responses for different lectins after decreasing the lectin concentration to 48 nM (Fig. 2b). These results showed that all lectins displayed excellent classification without any overlap (Fig. 2). The classification accuracy is 93.3% for 15 randomly unknown samples even in such low concentration (Table S6, ESM). Furthermore, the hierarchical clustering analysis (HCA) [27] was performed to validate the effectiveness of the results from the array. Unlike LDA, HCA is a model-free standard chemometric approach to cluster similar subjects

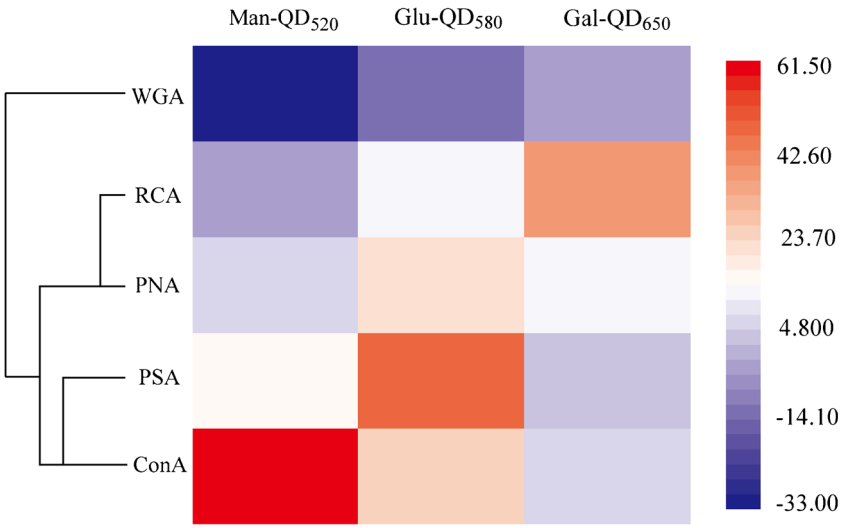

Fig. 3 Heat map of the signal patterns for the five lectins with concentration of 48 nM

into a group based on their spatial distances in full vector space. The average fluorescence response of each lectin was used to perform HCA and drawn heat map as Fig. 3. The differential response patterns in heat map demonstrated the high sensitivity of the s-QD/MoS_2 nanosheets array to different lectins. HCA produced several classes that were consistent with their affinities to saccharides (Table S2). These results indicated that the s-QD/MoS_2 nanosheets array was effective to reflect the characteristics of lectins, and thus was suitable for identifying different analytes even at lower concentration with high classification accuracy.

Quantitative analysis

After validating the ability of the fluorescent array for lectins identification, further studies were also performed to confirm whether this array can quantify the lectins. In this regard, ConA with different concentration as the model were tested on the fluorescent array. The two canonical factors were visualized as a 2D model with a classification accuracy of 100% (Table S7, ESM and Fig. 4a). According to the classified results of LDA, the canonical factors were 90.3% for factor (1) and 9.2% for factor (2). It is worth noting that factor (2) was much less than factor (1) and thus factor (1) was used to quantify the lectins. As shown in Fig. 4, this array was applied to detect lectins at different concentrations. The linearity of dose-response curves in Fig. 4b revealed that the concentration-dependent signal changes can be used for ConA quantitation ($R^2 = 0.997$). The limit of detection (LOD) of ConA is calculated to be 3.7 nM by $3\sigma/S$ (where σ is the standard deviation of the blank and S is the slope of the calibration plot). Likewise, the

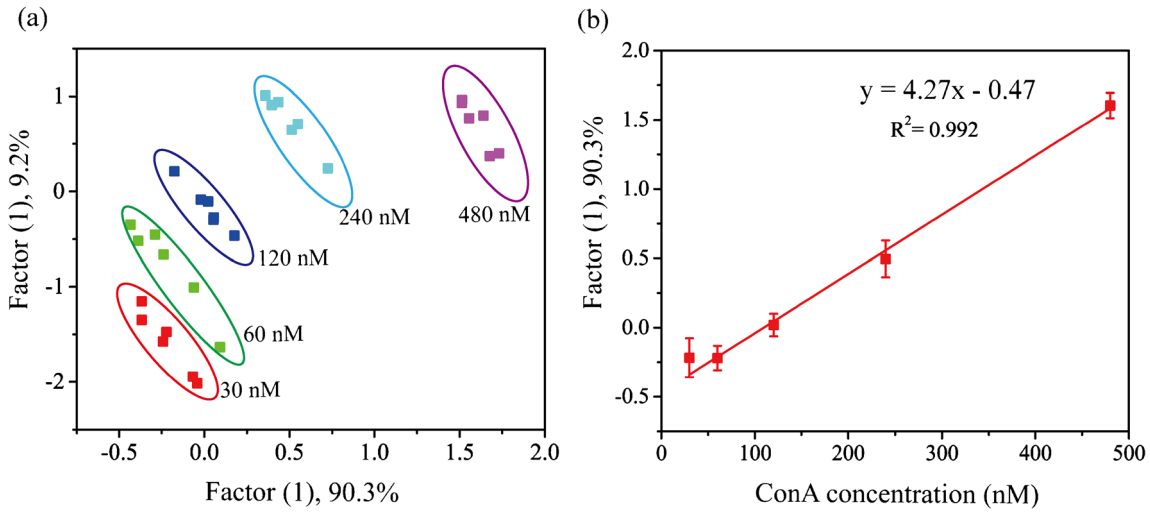

Fig. 4 Quantitation of ConA. **a** Canonical score plots of ConA with concentration of 10, 12.5, 25, 50, and 100 nM. **b** Linear fitting between Factor (1) and ConA, the error bars represent the standard deviation ($n = 6$)

Table 1 An overview on recently reported nanomaterials-based methods for lectins detection

Method applied	Material used	Analyte	LOD (nM)	Analysis mode	Reference
Fluorescence assay	QDs	ConA	100	One by one	[4]
Electrochemical assay	Gold nanowire	ConA	4–13	One by one	[5]
Raman scattering assay	Silver nanoparticles	ConA	78	One by one	[6]
Colorimetric assay	Sliver/gold nanoparticles	ConA	40	One by one	[7]
Colorimetric assay	Gold nanoparticles	ConA	9	One by one	[8]
Diffraction sensing	2D photonic crystals	ConA	38	One by one	[28]
Multichannel optical assay	Multiple QDs	Five lectins	4.9	Multiple detection	[29] (Our group)
Fluorescent array assay	QDs-MoS_2 nanosheet conjugates	Lectins and bacteria	3.7	Multiple detection	This work

quantitative analysis of PSA, PNA and RCA was also performed (Fig. S11 - Fig.S13, ESM) with LODs of 8.3, 4.2 and 3.9 nM, respectively. Additionally, this analytical method compared with other nanomaterial-based detecting methodologies for lectins are listed in Table 1. This method provided lower LOD value for simultaneous detection of multiple lectins.

Bacteria identification

The surface of bacteria contains different types and amounts of lectins that act as saccharide receptors to facilitate their recognition and adhesion [30, 31]. In this regard, bacteria can identify based on our method. The five bacteria (*E. coli, E. faecalis, E. faecium, S. aereus, and B. sublitis*) were selected as the models to verify the performance. As shown in Fig. 5, there are distinct fluorescence response patterns mainly due to the differential presence of lectins on the surface of bacteria [30, 32]. Then, the quantitation analysis of bacteria (*E. coli* and *E. faecium*) was further carried out with the fluorescent array. As shown in Fig. S14 and Fig. S15, the Factor (1) were corrected with the concentration of *E. coli* and *E. faecium* in range of 32–10^8 cfu mL^{-1}. The LOD of *E. coli* and *E. faecium* was calculated to be 87 cfu mL^{-1} and 66 cfu mL^{-1}, respectively. As rapid and efficient identification of multiple bacteria is an important issue in medical, forensic, and environmental sciences [11]. We further verified the real sample analysis ability of the fluorescent array by using milk as the matrix. As shown in Table S4 (ESM), the fluorescent array-based method for *E. coli* and *E. faecium* detection showed satisfactory.

Conclusion

In summary, a fluorescent array by employing green, yellow, and red light emitting s-QDs and PBA-MoS_2 nanosheets conjugates as signal probes is developed. This array successfully achieved simultaneous identification and quantitation of multiple lectins and bacteria with excellent accuracy and wide detection range. It holds great potential for the application in the

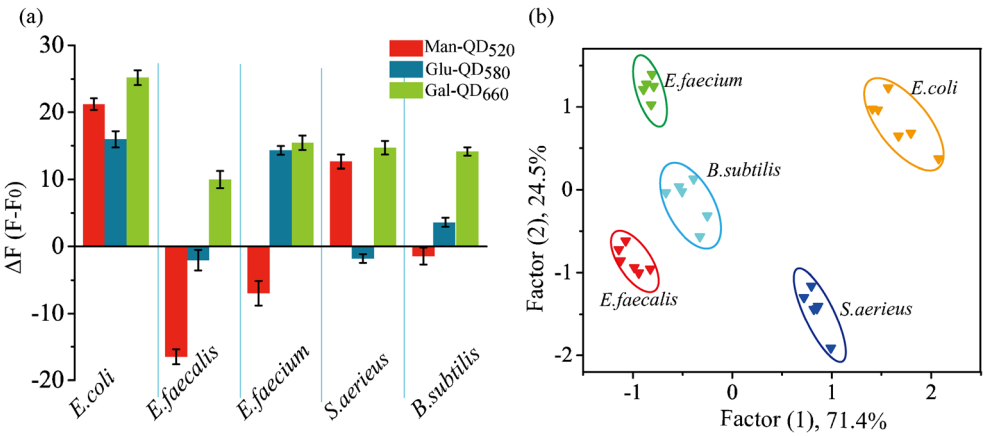

Fig. 5 Identification of different bacteria. **a** Fluorescence response patterns of the fluorescent array against 7×10^7 cfu mL^{-1} of bacteria, and (**b**) Canonical score plots of bacteria via LDA signal patterns. Five species microorganisms are *E. coli, E. faecalis, E. faecium, S. aereus,* and *B. sublitis*. **a** The error bars represent the standard deviation ($n = 6$)

detection of pathogens that possess lectins on their surface. On point to be mentioned that UV light (380 nm) was used as excitation wavelength in this work. Generally, bio-matrix can emit background fluorescence under UV excitation which may interfere the analysis result. However, this will not limit the application of this fluorescent array in clinical diagnostics and prognostics, because the statistical cross-reactive signal processing manner of the array-based methods is well-known for eliminating complex background interference. Besides, to apply fluorescent materials with longer excitation and emission wavelength in the construction of the arrays should be a new direction in this area.

Acknowledgements This work was financially supported by the National Natural Science Foundation of China (21675016) and the Fundamental Research Funds for the Central Universities (106112017CDJXFLX0014).

Compliance with ethical standards The author(s) declare that they have no competing interests.

References

1. Liu Z, Liu H, Wang L, Su X (2016) A label-free fluorescence biosensor for highly sensitive detection of lectin based on carboxymethyl chitosan-quantum dots and gold nanoparticles. Anal Chim Acta 932:88–97
2. Doores KJ, Gamblin DP, Davis BG (2006) Exploring and exploiting the therapeutic potential of glycoconjugates. Chem-Eur J 12:656–665
3. Disney MD, Seeberger PH (2004) The use of carbohydrate microarrays to study carbohydrate-cell interactions and to detect pathogens. Chem Biol 11:1701–1707
4. Ponnusamy Babu SS, and Avadhesha Surolia (2007) Sugar-Quantum Dot Conjugates for a Selective and Sensitive Detection of Lectins. Bioconjugate Chem 18:146–151
5. Bhattarai JK, Tan YH, Pandey B, Fujikawa K, Demchenko AV, Stine KJ (2016) Electrochemical impedance spectroscopy study of Concanavalin A binding to self-assembled monolayers of mannosides on gold wire electrodes. J Electroanal Chem 780: 311–320
6. Craig D, Simpson J, Faulds K, Graham D (2013) Formation of SERS active nanoparticle assemblies via specific carbohydrate-protein interactions. Chem Commun 49:30–32
7. Schofield CL, Haines AH, Field RA, Russell DA (2006) Silver and gold glyconanoparticles for colorimetric bioassays. Langmuir 22: 6707–6711
8. Watanabe S, Yoshida K, Shinkawa K, Kumagawa D, Seguchi H (2010) Thioglucose-stabilized gold nanoparticles as a novel platform for colorimetric bioassay based on nanoparticle aggregation. Colloid Surface B 81:570–577
9. Ferre S, Baler R, Bouvier M, Caron MG, Devi LA, Durroux T, Fuxe K, George SR, Javitch JA, Lohse MJ, Mackie K, Milligan G, Pfleger KDG, Pin JP, Volkow ND, Waldhoer M, Woods AS, Franco R (2009) Building a new conceptual framework for receptor heteromers. Nat Chem Biol 5:131–134
10. Lis H, Sharon N (1998) Lectins: Carbohydrate-specific proteins that mediate cellular recognition. Chem Rev 98:637–674
11. Sharon N (1987) Bacterial Lectins, Cell-Cell Recognition and Infectious-Disease. FEBS Lett 217:145–157
12. Otten L, Vlachou D, Richards SJ, Gibson MI (2016) Glycan heterogeneity on gold nanoparticles increases lectin discrimination capacity in label-free multiplexed bioassays. Analyst 141:4305–4312
13. Richards SJ, Otten L, Gibson MI (2016) Glycosylated gold nanoparticle libraries for label-free multiplexed lectin biosensing. J Mater Chem B 4:3046–3053
14. Hizir MS, Robertson NM, Balcioglu M, Alp E, Rana M, Yigit MV (2017) Universal sensor array for highly selective system identification using two-dimensional nanoparticles. Chem Sci 8:5735–5745
15. Freeman R, Willner I (2012) Optical molecular sensing with semiconductor quantum dots (QDs). Chem Soc Rev 41:4067–4085
16. Wang K, Dong Y, Li B, Li D, Zhang S, Wu Y (2017) Differentiation of proteins and cancer cells using metal oxide and metal nanoparticles-quantum dots sensor array. Sens Actuator B-Chem 250:69–75
17. Zhang F, Lu C, Wang M, Yu X, Wei W, Xia Z (2018) A Chiral Sensor Array for Peptidoglycan Biosynthesis Monitoring Based on MoS_2 Nanosheet-Supported Host–Guest Recognitions. ACS Sens 3:304–312
18. Zhu C, Zeng Z, Li H, Li F, Fan C, Zhang H (2013) Single-Layer MoS_2-Based Nanoprobes for Homogeneous Detection of Biomolecules. J Am Chem Soc 135:5998–6001
19. Yang Y, Liu T, Cheng L, Song G, Liu Z, Chen M (2015) MoS_2-based nanoprobes for detection of silver ions in aqueous solutions and bacteria. ACS Appl Mater Inter 7:7526–7533
20. Qu F, Liu Y, Kong R, You J (2017) A versatile DNA detection scheme based on the quenching of fluorescent silver nanoclusters by MoS2 nanosheets: Application to aptamer-based determination of hepatitis B virus and of dopamine. Microchim Acta 184:4417–4424
21. Knirsch KC, Berner NC, Nerl HC, Cucinotta CS, Gholamvand Z, McEvoy N, Wang Z, Abramovic I, Vecera P, Halik M, Sanvito S, Duesberg GS, Nicolosi V, Hauke F, Hirsch A, Colernan JN, Backes C (2015) Basal-plane functionalization of chemically exfoliated molybdenum disulfide by diazonium salts. ACS Nano 9:6018–6030
22. Yang Y, Zhao Y, Yan T, Yu M, Sha Y, Zhao Z, Li Z (2010) Design and fabrication of multivalent Gal-containing quantum dots and study of its interactions with asialoglycoprotein receptor (ASGP-R). Tetrahedron Lett 51:4182–4185
23. Lee RT, Lee YC (1974) Synthesis of 3-(2-Aminoethylthio)propyl glycosides. Carbohyd Res 37:193–201
24. Zu F, Yan F, Bai Z, Xu J, Wang Y, Huang Y, Zhou X (2017) The quenching of the fluorescence of carbon dots: A review on mechanisms and applications. Microchim Acta 184:1899–1914
25. Shinde S, El-Schich Z, Malakpour A, Wan W, Dizeyi N, Mohammadi R, Rurack K, Gjorloff Wingren A, Sellergren B (2015) Sialic acid-imprinted fluorescent core-shell particles for selective labeling of cell surface glycans. J Am Chem Soc 137: 13908–13912
26. Gorityala BK, Lu Z, Leow ML, Ma J, Liu X (2012) Design of a Turn-Off/Turn-On" biosensor: Understanding carbohydrate-lectin interactions for use in noncovalent drug delivery. J Am Chem Soc 134:15229–15232
27. Teixeira MR, Ribeiro FR, Torres L, Pandis N, Andersen JA, Lothe RA, Heim S (2004) Assessment of clonal relationships in ipsilateral and bilateral multiple breast carcinomas by comparative genomic hybridisation and hierarchical clustering analysis. Brit J Cancer 91: 775–782

28. Cai Z, Sasmal A, Liu X, Asher SA (2017) Responsive photonic crystal carbohydrate hydrogel sensor materials for selective and sensitive lectin protein detection. ACS Sens 2:1474–1481
29. Wang L, Zhang Y, He H, Yang H, Wei W (2018) Simultaneous quadruple-channel optical transduction of a nanosensor for multiplexed qualitative and quantitative analysis of lectins. Chem Commun 54:7754–7757
30. Luo PG, Wang H, Gu L, Lu F, Lin Y, Christensen KA, Yang S, Sun Y (2009) Selective interactions of sugar-functionalized single-walled carbon nanotubes with bacillus spores. ACS Nano 3: 3909–3916
31. Disney MD, Zheng J, Swager TM, Seeberger PH (2004) Detection of bacteria with carbohydrate-functionalized fluorescent polymers. J Am Chem Soc 126:13343–13346
32. Kuralay F, Sattayasamitsathit S, Gao W, Uygun A, Katzenberg A, Wang J (2012) Self-propelled carbohydrate-sensitive micro-transporters with built-in boronic acid recognition for isolating sugars and cells. J Am Chem Soc 134:15217–1522